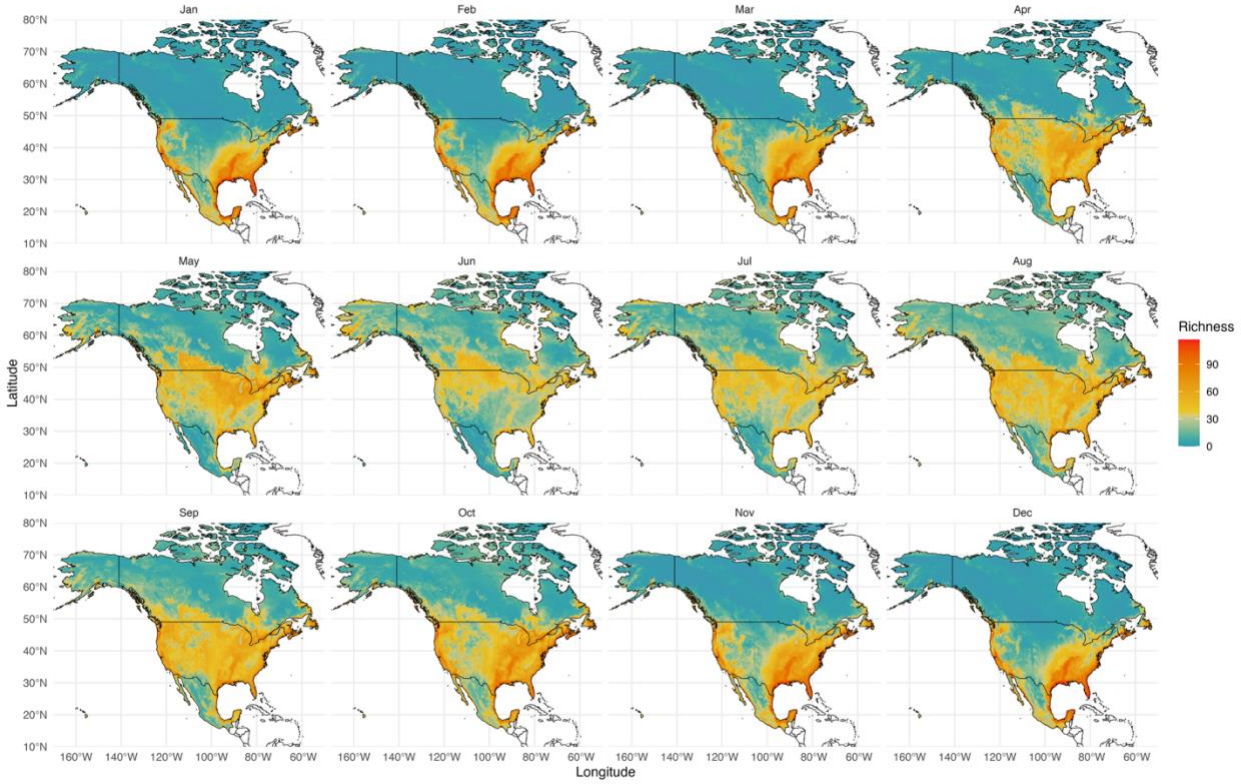

Figure S1. Monthly species richness maps for waterbird communities across North America (January-December). Consistent ecological hotspots are visible along the Prairie Pothole Region, Great Lakes basin, Atlantic Flyway (including the Delmarva Peninsula), and key coastal and wetland complexes of the Gulf of Mexico and Pacific Flyway. These spatial and temporal patterns reflect the dynamic migratory strategies of waterbirds and highlight regions of persistent ecological importance for avian diversity.

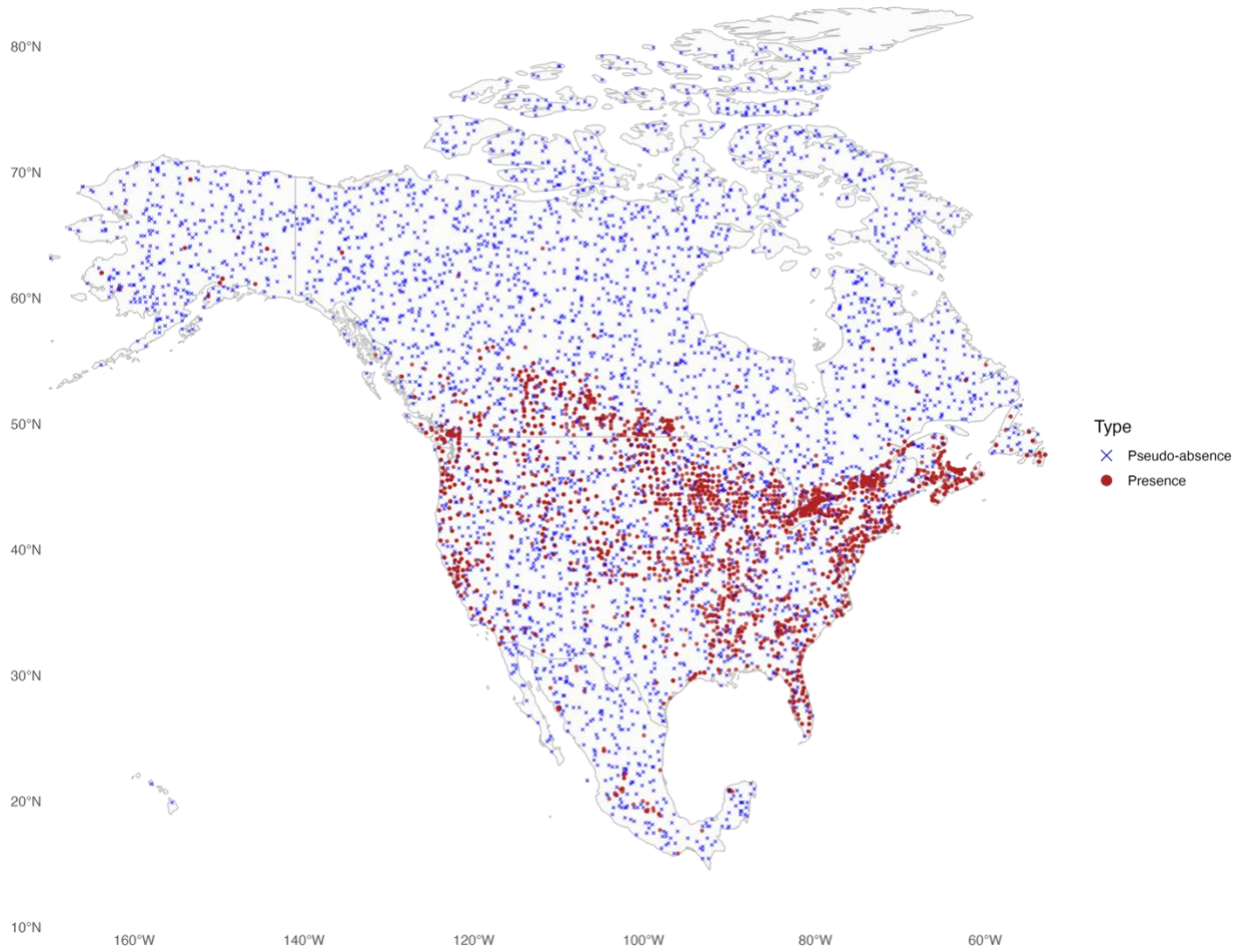

Figure S2. Confirmed HPAI presences (red circles) and pseudo-absence points (blue crosses) across North America. The study area was restricted to ecologically and anthropogenically

relevant zones defined by wild-bird diversity hotspots, high poultry and livestock densities, and human settlement rather than the entire continent. A 15 km buffer around each confirmed outbreak excluded areas of potential undetected infection, and pseudo-absences were then drawn by stratified random sampling within the remaining mask to match environmental conditions of the presences. Equal numbers of presence and pseudo-absence locations ensure balanced model calibration and reduce spatial bias.

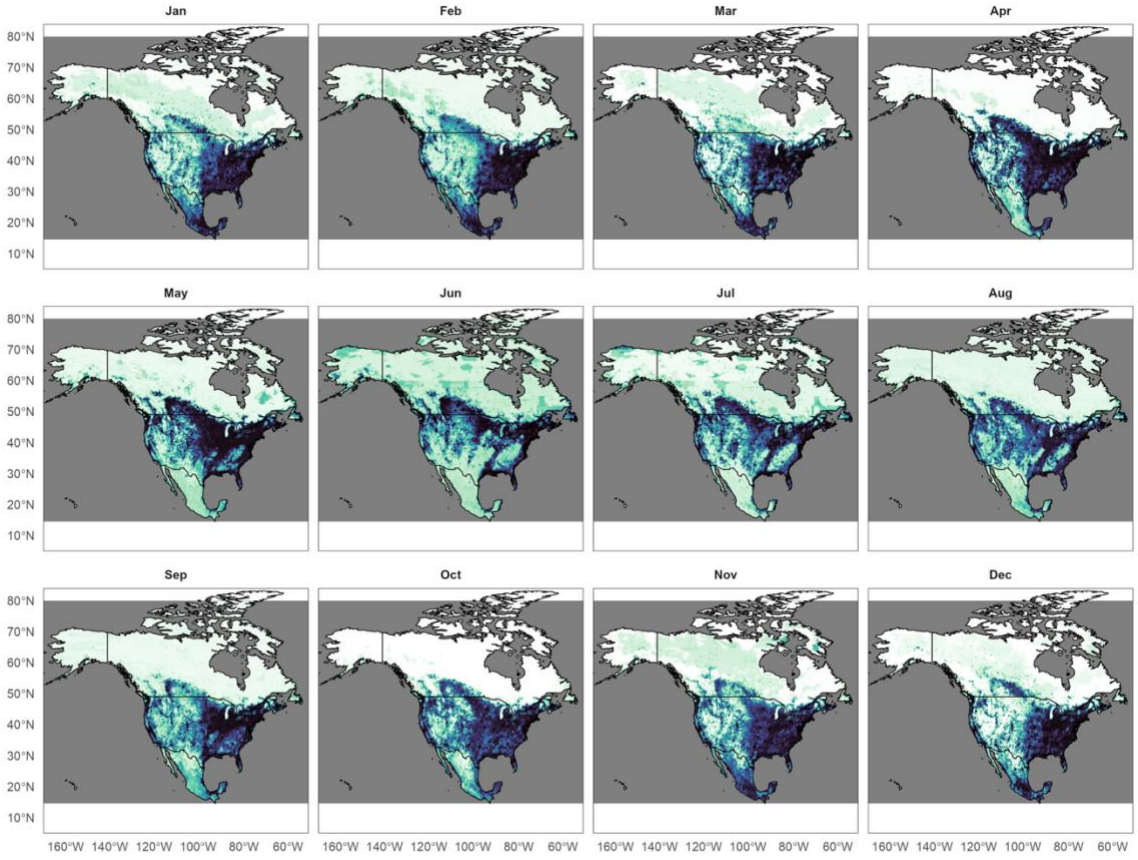

Figure S3. Continental-scale seasonality of HPAI risk derived from Hill-1 entropy. Monthly panels integrate 126 species models, revealing synchronized north-south oscillations in exposure potential consistent with large-scale migratory dynamics across North American flyways.

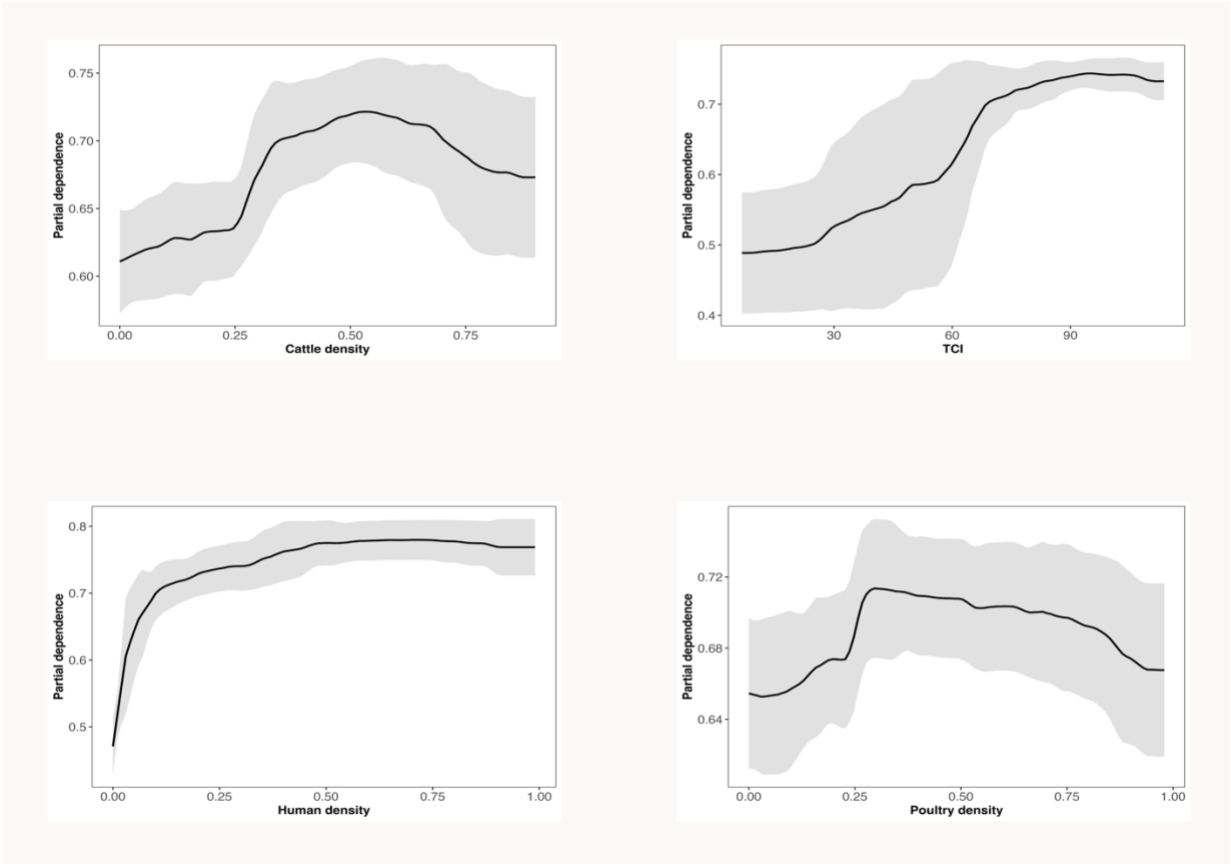

Figure S4. Mean partial dependence plots (PDPs) showing the averaged influence of human density, poultry density, cattle density, and TCI on predicted HPAI risk across all months. Solid lines represent the mean partial dependence of each variable, and shaded ribbons indicate month-to-month variability (±1 SD). Risk generally increases with higher human and TCI values,

peaks at intermediate poultry and cattle densities, and declines at the highest densities, reflecting nonlinear saturation effects in agro-ecological pressure zones.

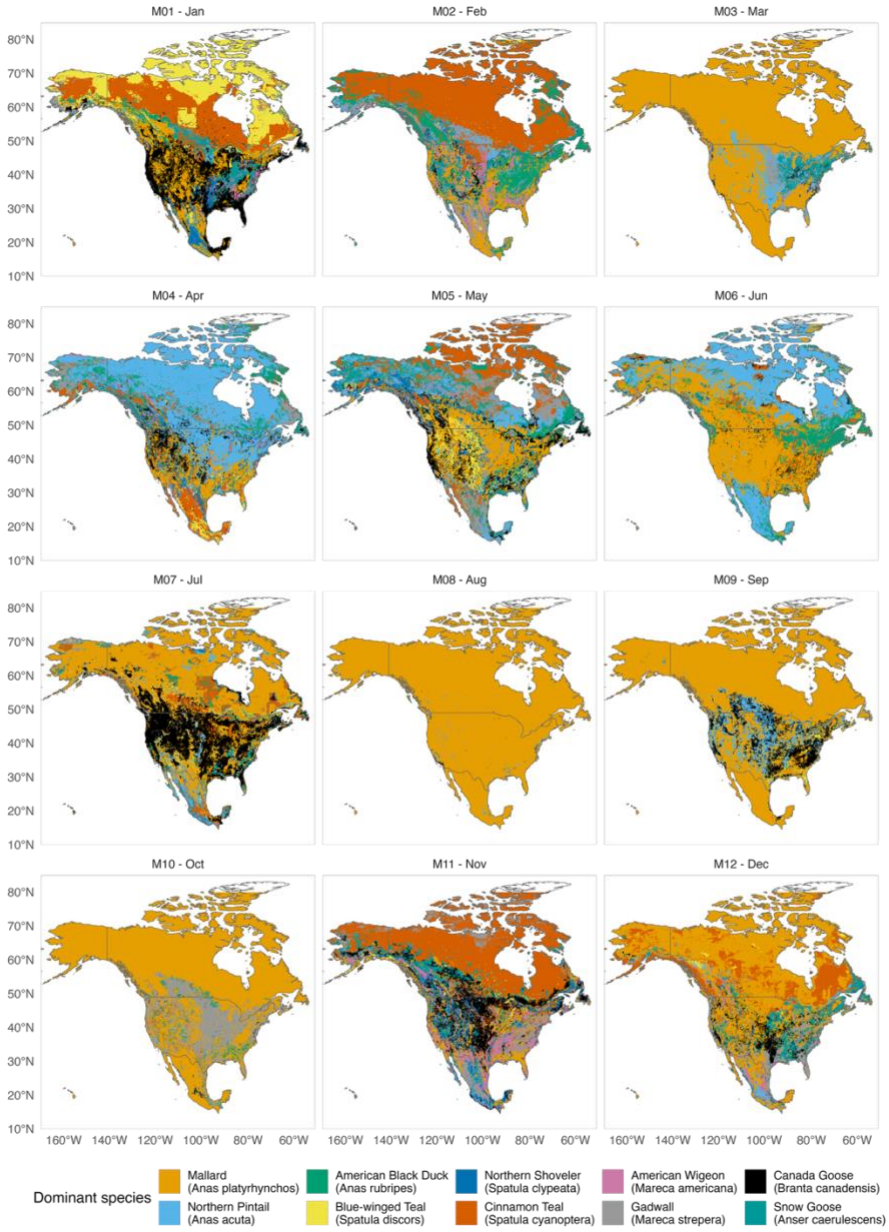

Figure S5. Monthly maps show the dominant waterfowl species contributing to modeled HPAI risk under the Hill-1 entropy framework. Each color represents the species with the strongest local effect based on Δ-probability between baseline and species neutralized predictions. Seasonal dominance tracks migration: Mallard and Northern Pintail dominate spring-fall flyways, Blue-winged Teal and Gadwall peak in summer wetlands, and Canada and Snow Goose prevail across northern wintering zones.

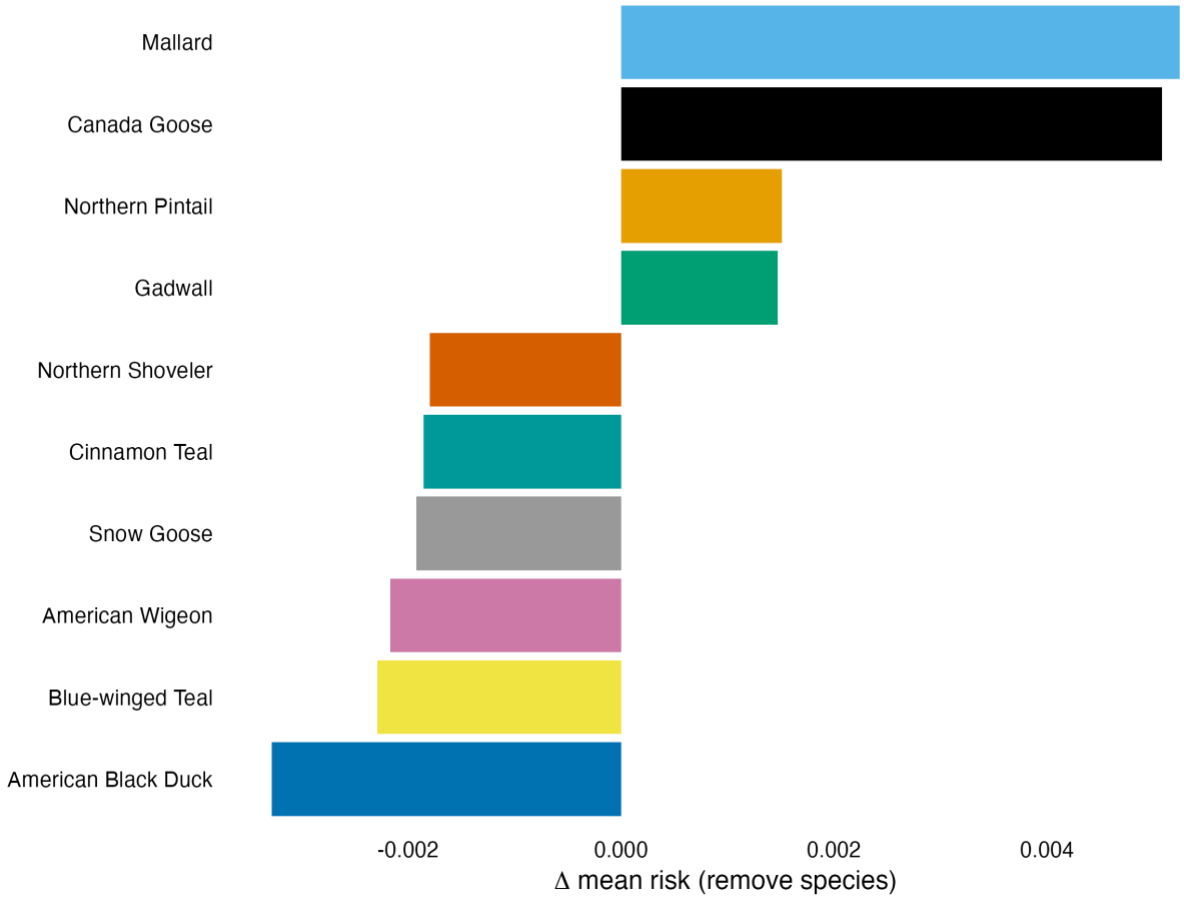

Figure S6. Leave-one-out sensitivity analysis: Relative reduction in risk when each focal species is excluded. Excluding Mallard, Canada Goose, Northern Pintail, or Gadwall yields the greatest relative reduction in modeled risk, whereas removing other dabblers produces moderate declines consistent with their secondary, context-dependent roles.

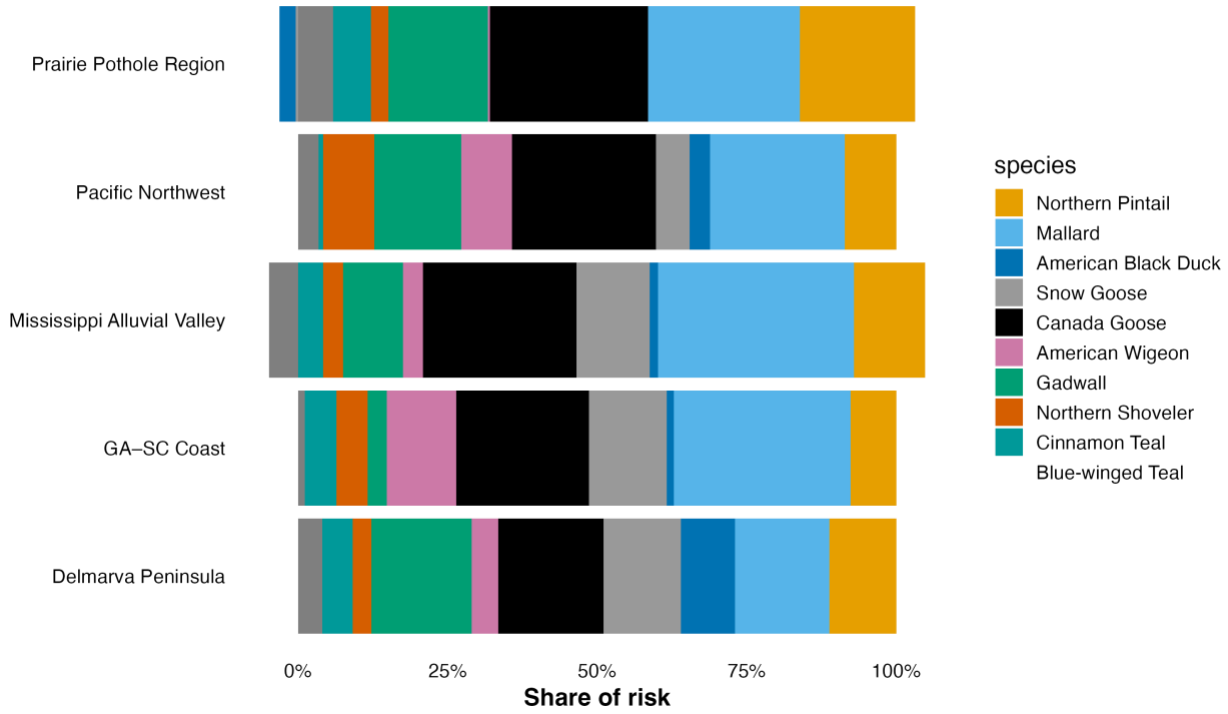

Figure S7. Regional species-level contributions to HPAI risk. Stacked bar plots show the proportional contribution of the ten focal waterfowl species to overall HPAI risk in each ecological hotspot. The Prairie Pothole Region and Mississippi Alluvial Valley exhibit balanced bars spanning many species-evidence of diffuse, community-level pressure. Delmarva, GA-SC, and the Pacific Northwest show higher concentration in fewer species, and the sensitivity bars mirror this by assigning disproportionately high marginal influence to the top four species.

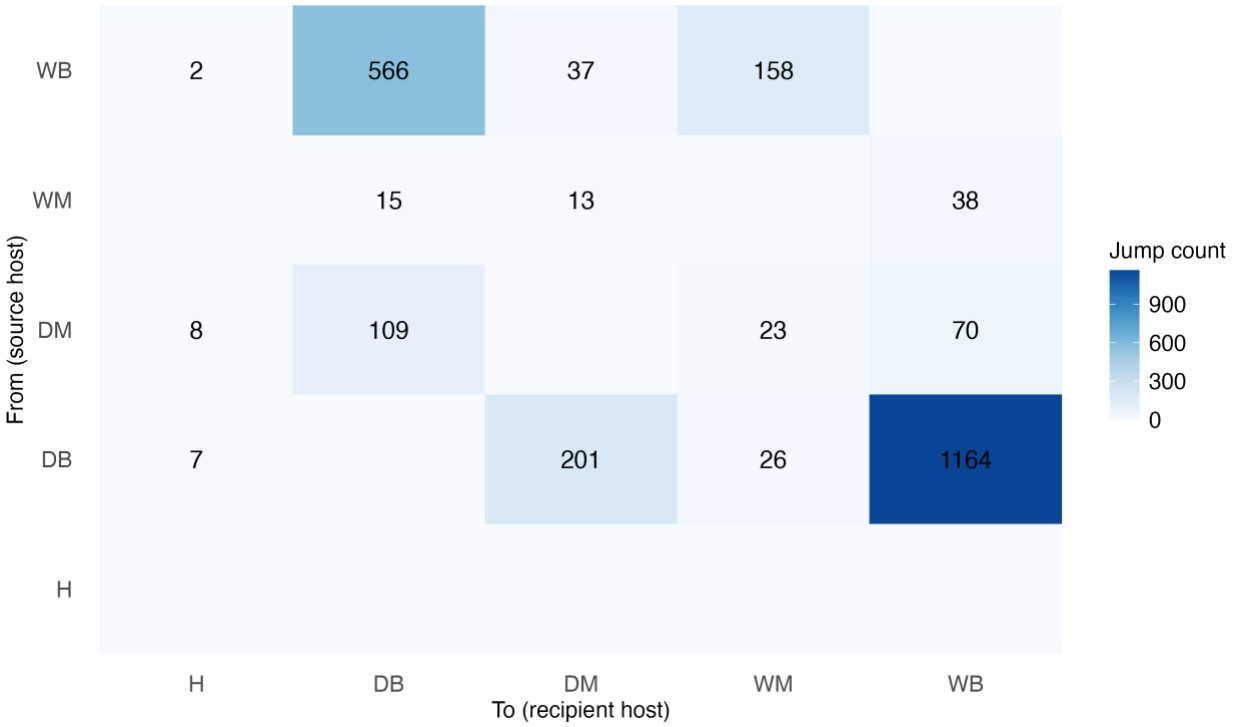

Figure S8. Cross-host transmission matrix of HPAI H5N1 (2021-2025) inferred from discrete-trait phylogenetic reconstruction. Matrix shows inferred transmission counts between major host categories: wild birds (WB), domestic birds (DB), wild mammals (WM), domestic mammals (DM), and humans (H). Values represent the number of reconstructed state transitions along internal branches of the time-scaled HA phylogeny (n = 14,263 sequences). Color intensity reflects the relative frequency of inferred events from carrier (rows) to recipient (columns). The analysis reveals that wild birds are the dominant source of transmission, particularly to domestic birds, while mammal-to-mammal and human-linked transitions are rare, indicating limited onward spread outside avian hosts.

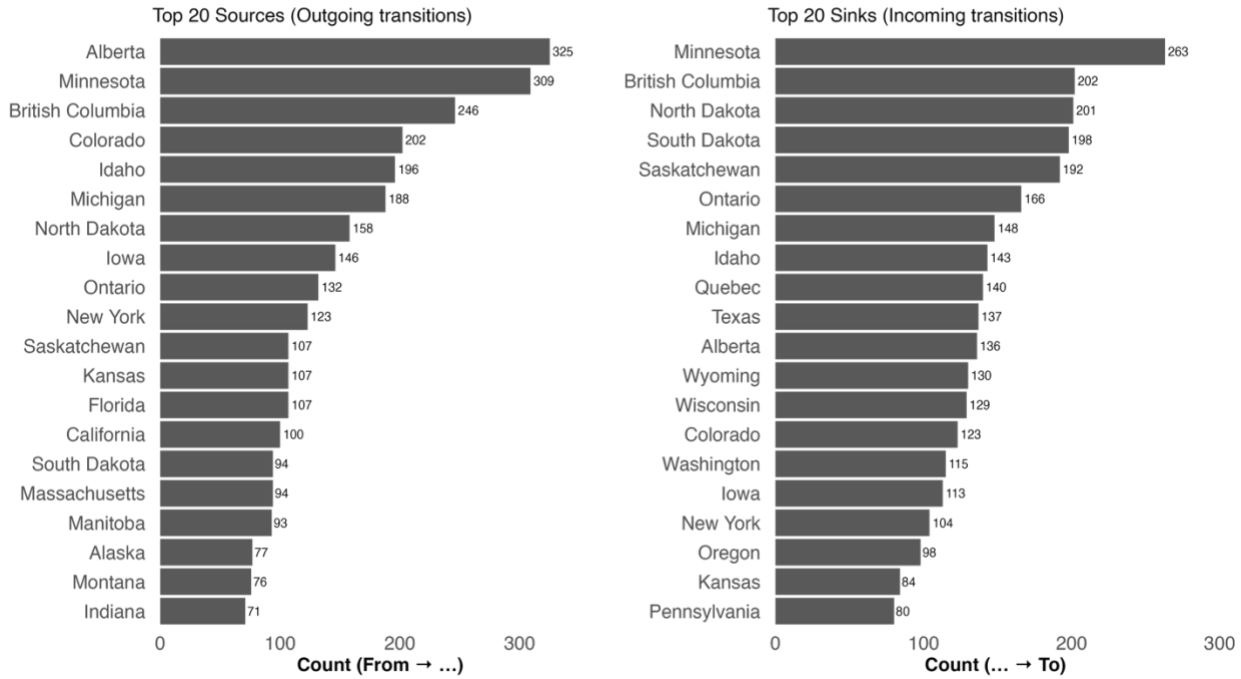

Figure S9. Top 20 geographic sources and sinks of HPAI H5N1 transmission events across North America (2021-2025). Bar plots show the 20 regions with the highest number of inferred viral transmissions acting as sources (left) and sinks (right), based on state- or province-level discrete trait reconstructions from the time-scaled HA phylogeny (n = 14,263 sequences). Source counts represent the number of inferred state transitions originating from each location, while sink counts represent transitions terminating in that location. The analysis highlights strong directional flow from western and central regions such as Alberta, Minnesota, and British Columbia, which served as major viral exporters, toward recipient regions in the Midwest, Great Lakes, and Atlantic corridors, reflecting migratory and poultry trade connectivity.

Figure S10. Time-scaled phylogeny of North American HPAI H5N1 viruses (2020-2025). Tips were colored by predicted spatial risk category (High = dark green, Medium = light green, Low = tan) from the integrated risk mapping framework. Tips represent full-length HA sequences, and branch colors indicate the most probable risk category at each node. The tree shows sustained diversification in high-risk regions from mid-2021, with intermittent introductions into medium- and low-risk areas.

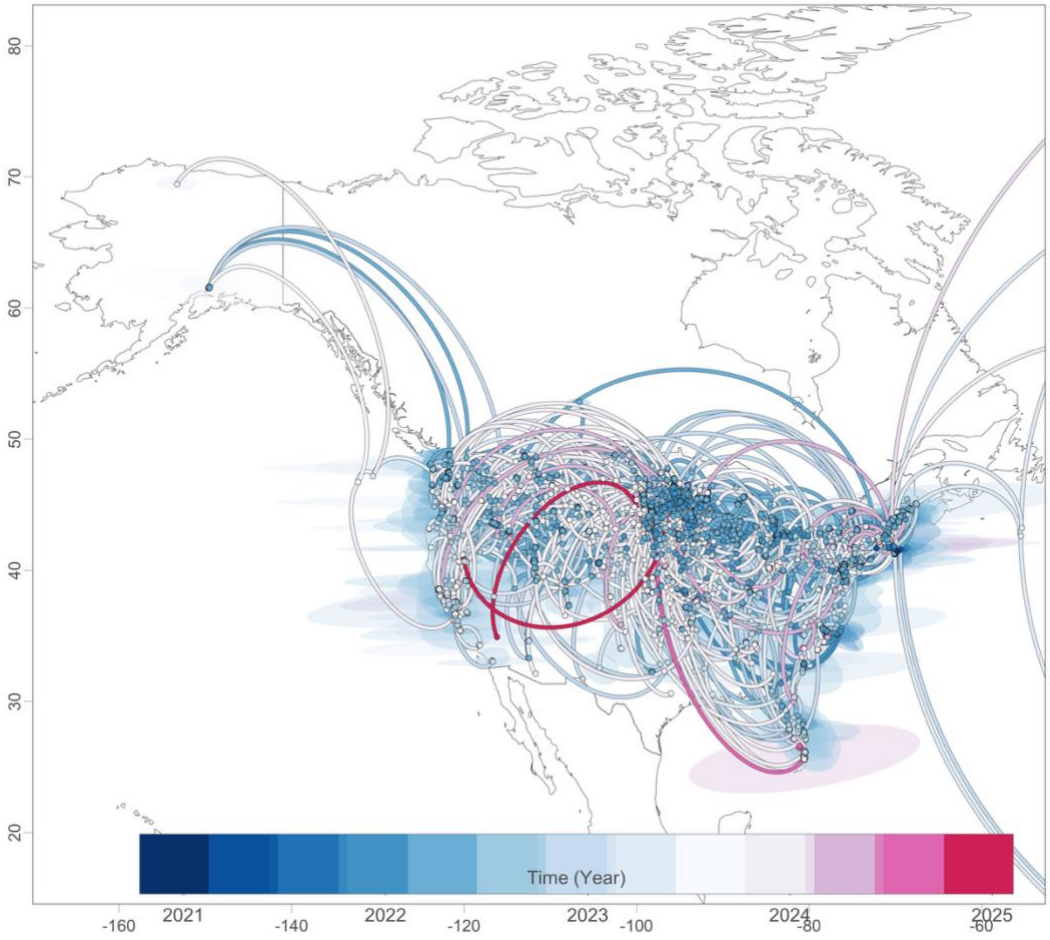

Figure S11. Continuous phylogeographic reconstruction of HPAI H5N1 diffusion across North America (2021-2025). The map depicts spatial dispersal inferred from a continuous trait analysis of 1,900 HA gene sequences, modeled under a relaxed random walk diffusion process. Lines represent inferred viral movement trajectories colored by time (dark blue: early 2021; red: late 2025). Spatial density shading indicates regions with the highest concentration of inferred transitions. The reconstruction reveals predominant north-south movements along major migratory flyways and recurrent reintroductions into the Prairie Pothole and Mississippi Valley regions, consistent with ecological hotspots identified in the risk mapping analysis.

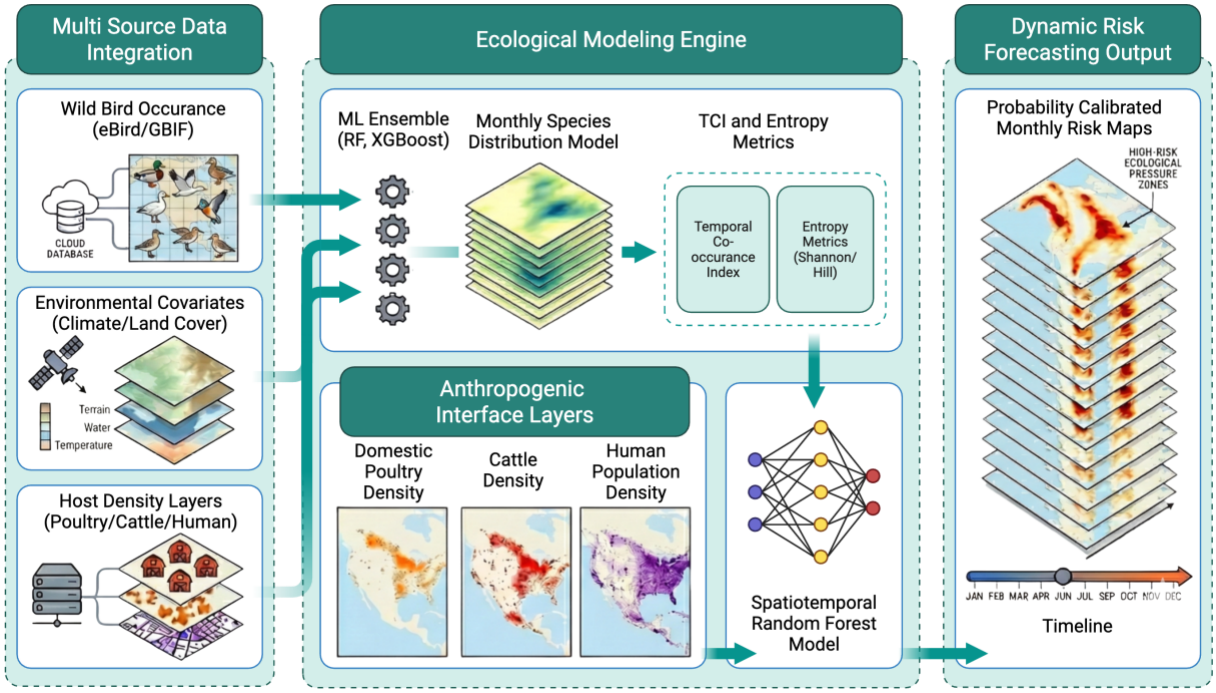

Figure S12. Workflow for dynamic HPAI risk forecasting. Multi-source inputs wild bird occurrence records (eBird/GBIF), environmental covariates (climate/land cover), and host-density layers (poultry, cattle, and humans) are integrated into an ecological modeling engine that generates monthly species distribution models using an ML ensemble (RF, XGBoost) and derives bird-aggregation metrics (Temporal Co-occurrence Index and Shannon/Hill entropy). These ecological predictors are combined with anthropogenic interface layers in a spatiotemporal Random Forest model to produce probability-calibrated, month-resolved risk maps that capture shifting ecological pressure zones across the annual cycle.